

Mesoscale Convective Systems over the United States during the 1997–98 El Niño

CHRISTOPHER J. ANDERSON AND RAYMOND W. ARRITT

Department of Agronomy, Iowa State University, Ames, Iowa

23 August 2000 and 2 April 2001

ABSTRACT

Large, long-lived mesoscale convective systems (MCSs) over the United States during the 1997–98 El Niño are documented. Two periods of abnormal MCS activity are identified in 1998: from March to mid-April an unusually large number of quasi-linear MCSs were observed in the Midwest; while quasi-circular MCSs in June–August of 1998 were concentrated near 37°N rather than following a seasonal shift similar to that observed in the climatological distribution. Episodic surges of northerly low-level flow were infrequent in March 1998, thereby leading to an unusually high incidence of quasi-linear MCSs and to precipitation anomalies in the central United States.

1. Introduction

A significant fraction of warm-season (Mar–Sep) precipitation in the central United States comes from mesoscale convective systems (MCSs), so that periods of anomalous MCS activity may result in abnormal precipitation patterns (Fritsch et al. 1986; Kunkel et al. 1994; Anderson and Arritt 1998). MCSs develop in regions of concentrated latent heat release as clusters of localized, convective storms merge and self-organize into precipitation systems of larger spatial dimension. Although the convective storms are local phenomena, the processes that control MCS development are observed over meso- to continental scales and from hourly to monthly periods (see, e.g., Mo et al. 1997; Maddox 1983). Thus, the distribution of MCSs varies with the large-scale condition (Augustine and Howard 1988, 1991; Anderson and Arritt 1998).

A process external to the United States that is capable of influencing the large-scale circulation over the United States is the El Niño–Southern Oscillation (ENSO). El Niño and the Southern Oscillation are quasi-regular changes in tropical Pacific sea surface temperature (SST) and surface pressure, respectively. The two fields are anticorrelated so that during an El Niño event an extensive pool of warm SST anomalies is overlaid by below average surface pressure (Montroy 1997). ENSO is the driving process for much of the interannual variability of precipitation in the tropical Pacific, because

the location of warm SST determines regions of tropical convection [for a more complete summary of ENSO see Trenberth (1997)]. Precipitation in the extratropics is influenced by ENSO through a less direct mechanism. Persistent upper-level outflow from tropical convection in the central and eastern equatorial Pacific during an El Niño event can initiate a chain of alternating regions of upper-level divergence and convergence that extend into mid- and high latitudes (Horel and Wallace 1981; Sardeshmukh and Hoskins 1988; Rasmussen and Mo 1993) and may affect the position of the time-mean extratropical jet stream and storm tracks. The position of the time-mean extratropical jet stream and storm tracks, in turn, affects the distribution of precipitation in the central United States.

Studies that have examined linkages between anomalies of equatorial Pacific SST and of central U.S. precipitation have focused mostly on time-mean quantities. They have found that, on average, an increase in rainfall in an area extending from northern Texas into the Dakotas is observed during April through October as warm equatorial Pacific SST anomalies increase in coverage (Ropelewski and Halpert 1986, 1987, 1989, 1996; Montroy 1997; Ting and Wang 1997; Bunkers et al. 1996). Precipitation is sometimes above average in the western Great Plains the following spring (Ropelewski and Halpert 1996; Montroy 1997). These studies were designed for the purpose of discovering repetitive patterns in both accumulated precipitation and the large-scale atmospheric fields. This strategy is unable to examine the episodic nature of precipitation and its dependence on regional weather systems. MCS summaries contain such information and are a natural complement to the aforementioned body of statistical research. However, be-

Corresponding author address: Christopher J. Anderson, Department of Agronomy, Iowa State University, 3010 Agronomy Hall, Ames, IA 50011-1010.
E-mail: candersn@iastate.edu

TABLE 1. MCC and PECS definitions.

Size	Continuous cloud shield (IR temperature $\leq -52^{\circ}\text{C}$) must have an area $\geq 50\,000\text{ km}^2$
Initiation	Size definition first satisfied
Duration	Size definition must be met for a period $\geq 6\text{ h}$
Maximum	Continuous cloud shield (IR temperature $\leq -52^{\circ}\text{C}$) reaches maximum size
Shape	MCC: minor axis/major axis ≥ 0.7 at maximum PECS: $0.2 \leq$ minor axis/major axis < 0.7 at maximum
Termination	Size criterion no longer satisfied

cause MCS summaries rely on satellite information, the length of the data record is much smaller than that of the statistical studies. Here we contribute a summary of MCS activity during the warm seasons of the extraordinary El Niño event in 1997–98.

2. Data sources

a. GOES-8 IR

Cloud-top characteristics of large, long-lived MCSs in *GOES-8* infrared (IR) digital satellite imagery were cataloged for March–September of 1997–98 with a modified version of the cloud-top documentation procedure developed by Augustine (1985). A more complete description of the routine is provided in Anderson and Arritt (1998). Hourly satellite data were obtained from the archive maintained by the Space Science and Engineering Center at the University of Wisconsin. From March through May of 1997, hourly *GOES-8* IR images were missing from 0400 to 0700 UTC on many

days. This has influenced our tabulation by creating some uncertainty in the time of maximum cloud-top area of events that occurred in this time frame. We viewed satellite imagery for each case to avoid including non-convective cloud shields, such as cirrus cloud streaks, and consulted surface station reports for cases that were ambiguous.

Each MCS documented by the automated routine was categorized as either quasi-circular or quasi-linear. Following previous summaries, we labeled a quasi-circular MCS as a mesoscale convective complex (MCC) and a quasi-linear MCS as a persistent elongated convective system (PECS). The formal criteria for these definitions are provided in Table 1. Note, first, that the duration and size criteria were devised by Maddox (1980) to indicate that these MCSs are likely to be organized on scales greater than those of convective storms and, second, that the shape criterion is applied only at the time of maximum extent.

b. Seasonal precipitation

Climate division monthly precipitation was obtained from the National Climate Data Center (NCDC). There are at most 10 climate divisions within each state. Monthly averages of precipitation are computed by NCDC for each division by equally weighting the monthly total precipitation at stations that consistently report both precipitation and temperature. NCDC requires the inclusion of both surface variables over a long time period as a quality control measure. We have averaged the monthly values for each division to obtain

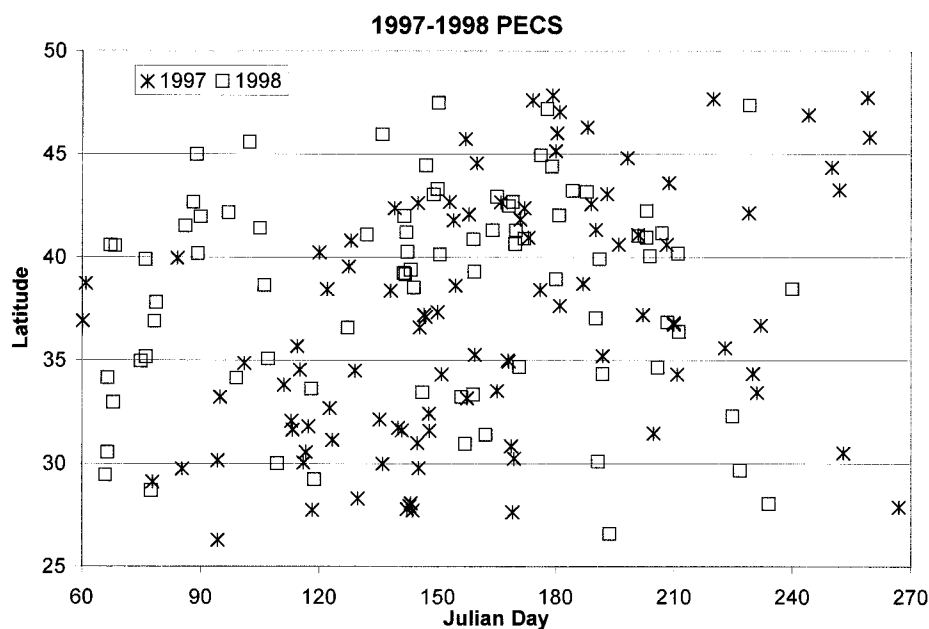


FIG. 1. Latitude–time distribution of -52°C cloud shield centroid at initiation for PECS in 1997 (stars) and 1998 (open squares).

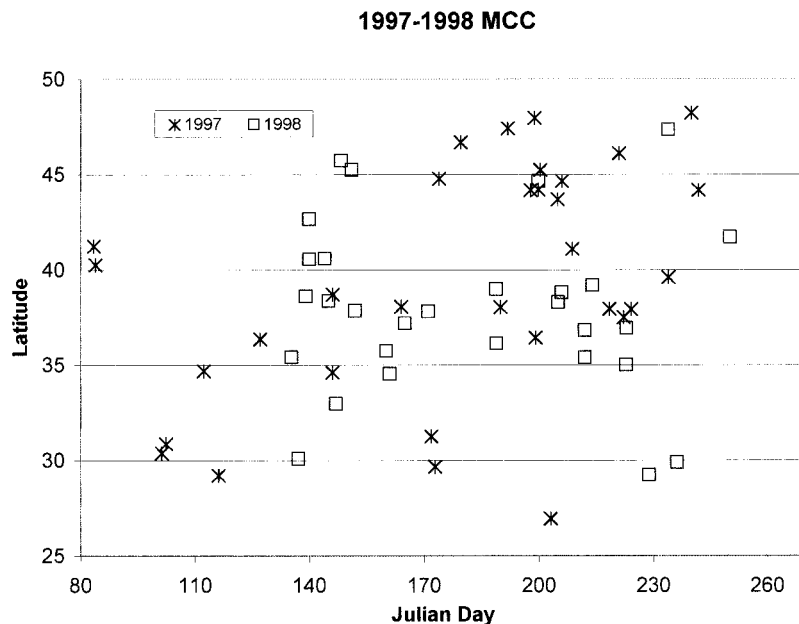


FIG. 2. Latitude–time distribution of -52°C cloud shield centroid at initiation for MCC in 1997 (stars) and 1998 (open squares).

seasonal values for March–April–May and June–July–August. For presentation purposes we have interpolated these data from irregular-spaced positions to a latitude–longitude grid with nodes equally spaced 2° apart. Our analysis scheme is based on Barnes (1964) and is performed with a single pass and an e -folding distance set equal to one grid length. These parameters were selected because our main interest is broad regional trends rather than local details. We computed anomalies from the 20-yr period 1979–98.

c. Microwave wind profilers

Hourly wind data from the the National Oceanic and Atmospheric Administration Wind Profiler Network (NPN) were categorized according to a wind speed threshold applied at low levels. NPN wind speed profiles that contained maximum speed $\geq 12 \text{ m s}^{-1}$ in the lowest 1500 m were labeled wind events (Mitchell et al. 1995). In order to ensure adequate sampling of the low-level wind, profiles were included only if four out of five levels below 1500 m were available. Daniel et al. (1999) and Arritt et al. (1997) found that NPN wind speed errors (Stensrud 1996) influenced the frequency of detection mainly for higher speed thresholds, so that such errors are less likely to influence the results herein.

3. Results and discussion

a. Overview of 1997–98 El Niño

The 1997–98 El Niño was unique in a number of ways. The onset of this event occurred in March 1997,

well before the typical onset for El Niño events (Wolter and Timlin 1998). The event intensified unusually rapidly. It reached the highest intensity at the earliest date yet to be recorded and maintained that level of intensity through December 1997, as the warm SST anomaly moved and expanded eastward into the central equatorial Pacific (McPhaden 1999; Wolter and Timlin 1998). The demise of the event occurred in mid-May 1998 and was as sudden as its onset, ending with a dramatic reversal of SST anomalies from positive to negative values along the coastline of Ecuador and Peru. McPhaden and Xu (1999) noted that the cooling rate at one location during the demise of this event was 10 times the normal cooling rate. Since 1950, only the El Niño event of 1982–83 was comparable in intensity to that of 1997–98 (Wolter and Timlin 1998).

Upper-tropospheric conditions over the extratropics were influenced by tropical convection in the central equatorial Pacific earlier than is usual during El Niño events (Barnston et al. 1999). Anomalous seasonal troughs were established off the United States west coast and over the southeastern United States from the fall of 1997 through the spring of 1998 (Bell and Halpert 1998; Bell et al. 1999). During this time the subtropical jet stream was abnormally strong and active (Bell et al. 1999). Above average precipitation was observed in the western and southern United States during November 1997–April 1998 and in the Midwest during spring of 1998. A sudden northward shift of the subtropical ridge in mid-May 1998 caused

an abrupt northward displacement of the jet stream over the central United States that persisted through the summer months, resulting in record drought and heat over the southern United States (Bell et al. 1999). This evolution was unexpected and highly atypical; in fact Barnston et al. (1999) note that previous examples of such behavior are nonexistent. However atypical it may have been, the final stages of this El Niño were likely to have contributed to the displacement of the jet stream as equatorial convection moved eastward with the SST anomalies, creating a shift in the upper-level convergence that may have led to ridging in the upper troposphere over the central United States (Bell et al. 1999; Barnston et al. 1999).

b. Latitude–time distribution of MCS centroid positions at initiation

1) PECS

The PECS populations for 1997 and 1998 are about the same size in each year and exhibit similar spatial patterns in summertime (Fig. 1; additional information for each PECS is provided in appendix Table A1). In particular, PECSs are most frequent during May and June (Julian days 121–181), when the average position of initiation is near 40°N. Similar seasonal characteristics are described in other MCS climatologies. In particular, Bartels et al. (1984) find that large cloud lines and hybrid systems, which correspond roughly to PECS, are most frequent from May into early June, and those in June are generally positioned north of those in May. Anderson and Arritt (1998) document a similar seasonal shift for PECS in 1992 and 1993. Noticeable differences between 1997 and 1998 are evident during March and April (Julian days 60–121). PECSs in March 1998 outnumber those in March 1997, while the reverse is true for April (Table A1). In addition, many events in March–April 1998 occur north of 40°N, whereas in 1997 nearly all events remain south of 40°N until late April (about Julian day 114), when a sudden increase in frequency is observed.

The uniqueness of the March 1998 PECS distribution is difficult to assess, since the number of satellite-based climatologies is small. Bartels et al. (1984) provides a relatively long record (1979–83) of MCS activity, and from this a comparison of MCS statistics in April is facilitated. Of the seven events in early April 1998 (Julian days 91–110), four PECS are positioned within the STORM-Central domain. For the years 1979–83 the frequency of large cloud lines and hybrid systems is similar only in April of 1981; however, large data gaps are present in April of 1979 and 1982 (Bartels et al. 1984). In neither 1992 nor 1993 was PECS frequency in March close to that of 1998, although early April of 1992 was nearly as active as early April of 1998 (Anderson and Arritt 1998). The suggestion from this small climatology is that a high incidence of large,

quasi-linear MCS in the central United States during March and early April may be rare.

2) MCC

MCC distributions differ substantially between 1997 and 1998 (Fig. 2; more information about each MCC is provided in Table A2). The MCC distribution for 1997 contains a northward shift in the mean position of initiation and an increase in frequency during July and August. In contrast, the 1998 distribution is defined by two space–time clusters, a springtime cluster from mid-May (Julian day 140) through mid-June (Julian day 170) and a late summer cluster from late July (Julian day 205) through late August (Julian day 240). Both clusters contain about the same number of events and are spread about 37°N so that a seasonal shift is not apparent. Other MCC summaries have documented a northward shift in position and maximum frequency in July (e.g., Augustine and Howard 1991). The 1997 distribution is quite typical in this regard; even the total number of MCCs (32) is nearly equal to that of the annual average (33). While MCCs in 1998 are almost as frequent (29) as in 1997, the space–time distribution is atypical.

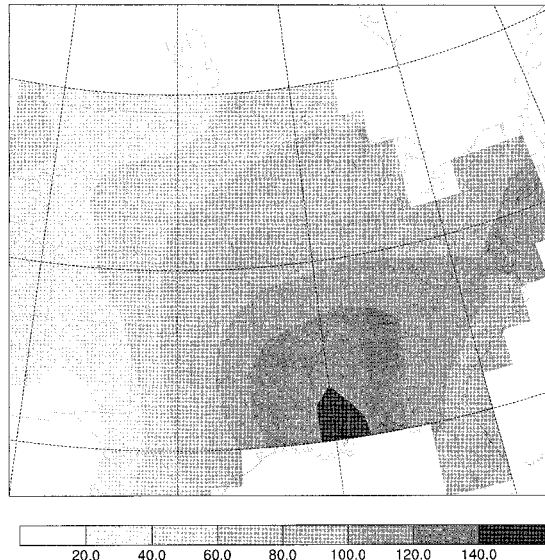
A persistent, large-scale ridge dominated the anomalous, large-scale circulation over the central United States at all levels from May through August of 1998 (see section 3a), along the periphery of which MCCs formed and propagated. Similar behavior is reported in Rodgers et al. (1985) and Augustine and Howard (1988, 1991) for MCCs in the central United States and Velasco and Fritsch (1987) and Laing and Fritsch (1997) for other regions of the world. It is curious that an anomalous northward shift of the mean position of MCCs occurred during the demise of El Niño events in both 1983 and 1998. While these two El Niño events are extraordinary and may not be representative of El Niño events in general, it is possible that they are cases in which equatorial convection influenced the distribution of summertime precipitation in the central United States.

c. Precipitation anomalies

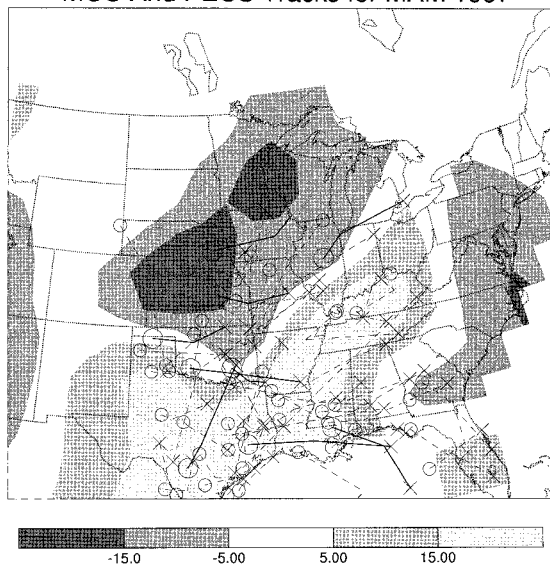
We have related seasonal precipitation to episodes of heavy precipitation by superimposing MCS tracks onto seasonal precipitation anomaly maps. We have constructed PECS and MCC tracks from the positions of the –52°C cloud centroids at the time of initiation, maximum, and termination.

A precipitation maximum in the 20-yr mean for March–May is located in the southeastern United States (Fig. 3a). Mean precipitation decreases to the west and north of the maximum. Anomaly maps for 1997 and 1998 contain opposite north–south dipole patterns in the central United States (Figs. 3b and 3c). However, the maps share a common trait. That is, positive anomalies in the central United States are coincident with densely

(a)
Climate Division MAM Mean Precipitation
1979-1998



(b)
Climate Division 1997 MAM Deviation Precipitation
MCC And PECS Tracks for MAM 1997



(c)
Climate Division 1998 MAM Deviation Precipitation
MCC And PECS Tracks for MAM 1998

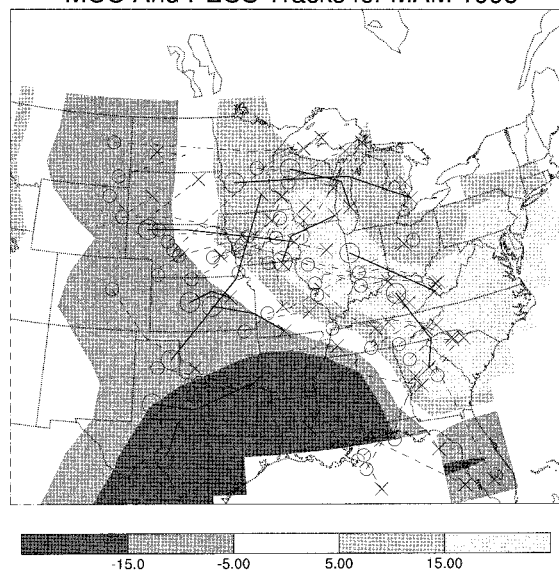


FIG. 3. Climate division precipitation (cm) for Mar–Apr–May (a) 20-yr mean (1979–98), (b) anomaly in 1997, and (c) anomaly in 1998. Overlaid on the anomaly maps are tracks of -52°C cloud shield centroid based on the position at initiation, maximum, and termination for each MCC (solid) and PECS (dashed).

spaced PECS and MCC tracks, while negative anomalies occur where PECSs and MCCs are relatively infrequent.

The primary maximum in mean precipitation for June–August is located in Florida, and mean precipitation decreases northwestward until a secondary maximum in the Great Plains (Fig. 4a). As in March–May

positive (negative) anomalies in the central United States for both 1997 and 1998 occur where PECSs and MCCs are frequent (infrequent). The abrupt onset and northward shift of the PECS distribution during May and June of 1997 is evident in the MCS tracks (Figs. 1 and 2), which display a minimum in MCS activity that is collocated with a negative precipitation anomaly over

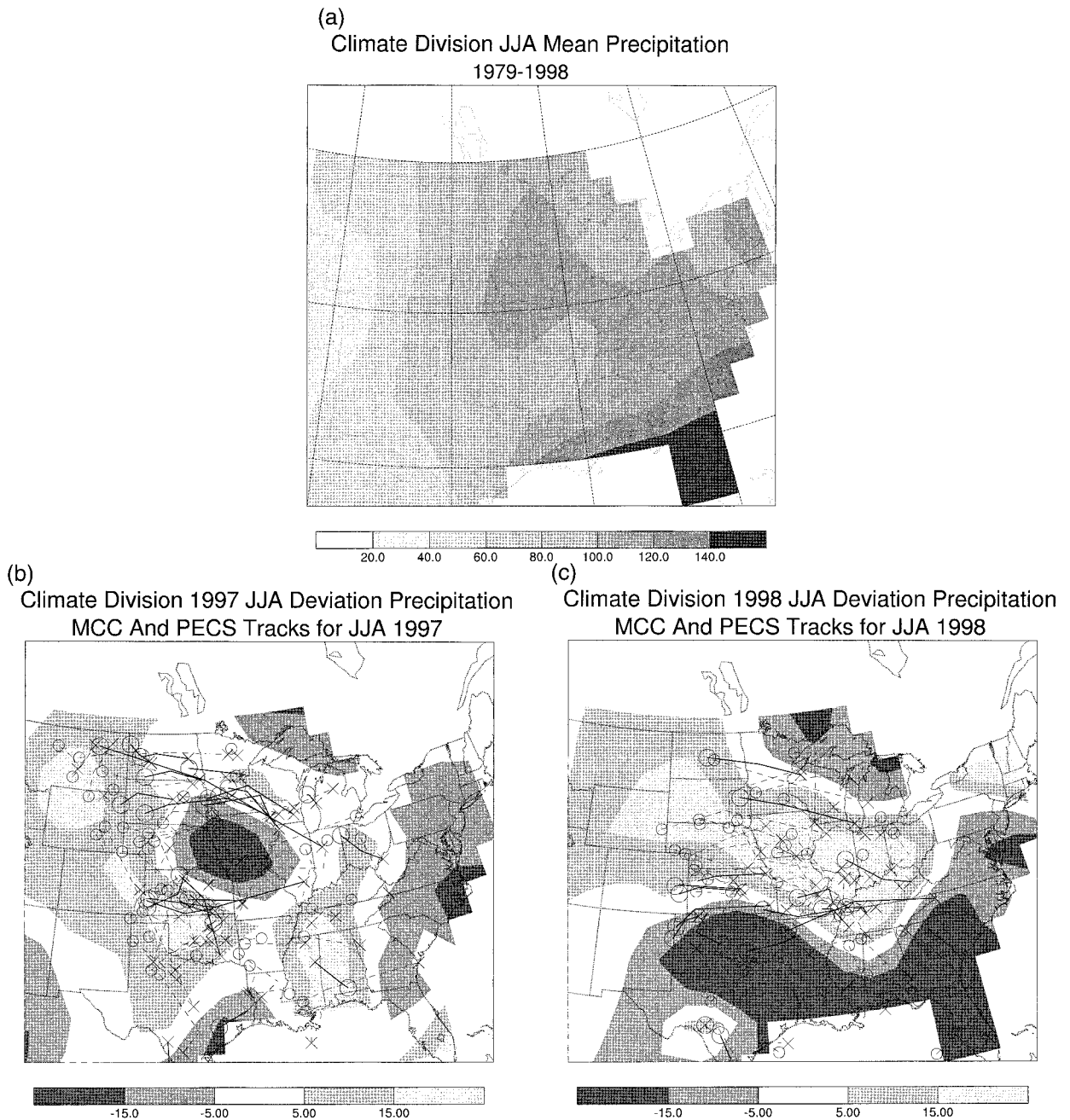


FIG. 4. Climate division precipitation (cm) for Jun–Jul–Aug (a) 20-yr mean (1979–98), (b) anomaly in 1997, and (c) anomaly in 1998. Overlaid on the anomaly maps are tracks of -52°C cloud shield centroid based on the position at initiation, maximum, and termination for each MCC (solid) and PECS (dashed).

much of the Midwest. In 1998, areas of positive and negative anomalies are more coherent and extensive (Fig. 4c), due to the persistent upper-level ridge. The position of the mean ridge periphery is reflected in the PECS and MCC tracks as a preponderance of tracks north of 35°N (Figs. 1 and 2).

A correspondence between central U.S. precipitation and MCS activity has been noted in other MCS sum-

maries. During the summertime drought in the central United States in 1983, quasi-circular MCSs were infrequent and were displaced northward of the central United States into a region where atmospheric water vapor is less abundant, thereby reducing the precipitation efficiency of the quasi-circular MCSs (Rodgers et al. 1983, 1985; Fritsch et al. 1986). In contrast, the high incidence of large MCSs, both quasi-linear and

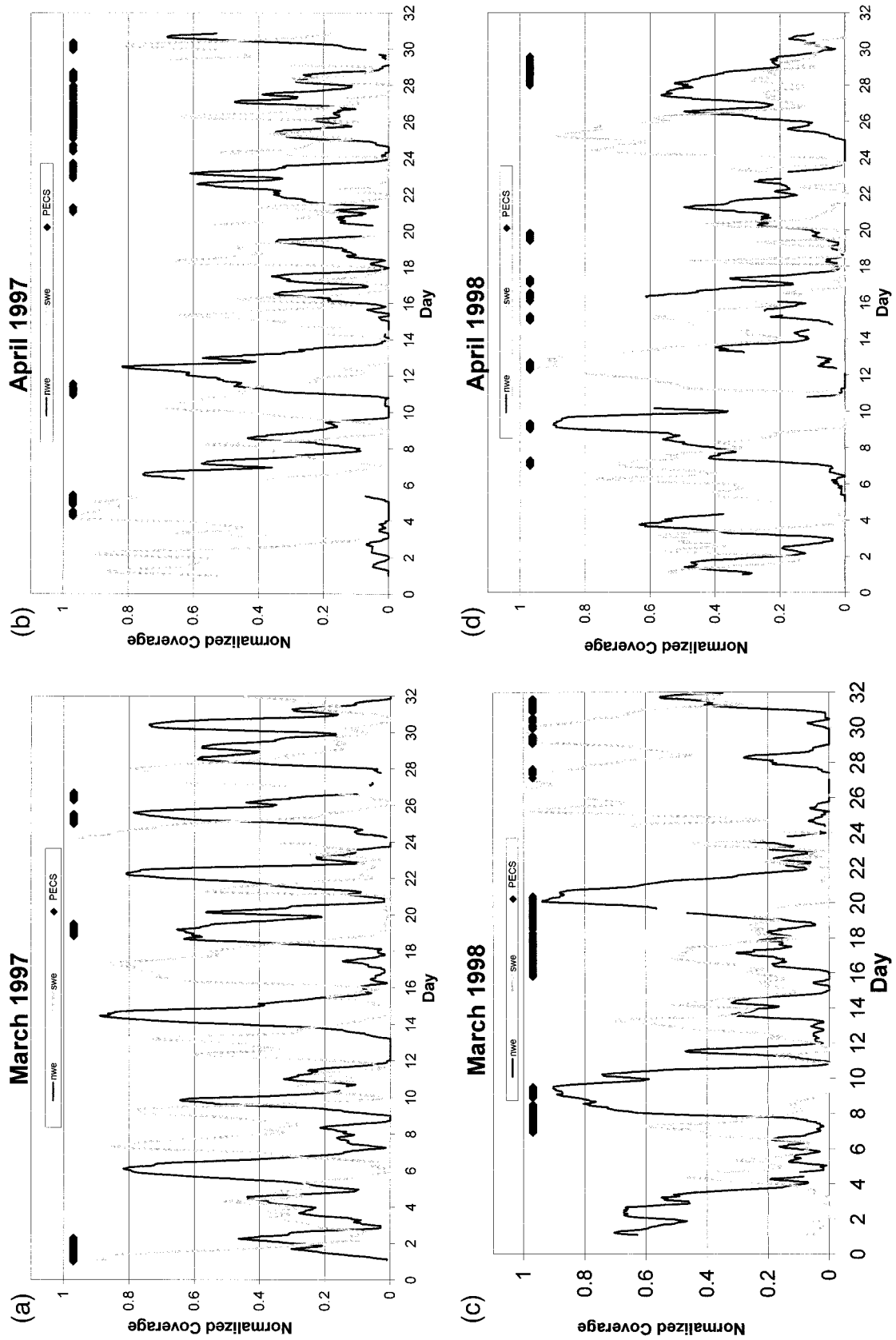


FIG. 5. Time series of northerly and southerly wind event normalized coverage for (a) Mar 1997, (b) Apr 1997, (c) Mar 1998, and (d) Apr 1998. Gaps in the time series indicate periods when less than half of the stations reported. Diamonds above the time series mark ongoing PECSs.

quasi-circular, over the central United States was an important factor in the development of the Midwestern flood in the summer of 1993 (Kunkel et al. 1995; Anderson and Arritt 1998). Compared with previous MCS summaries, the correspondence between positive precipitation anomalies and large, quasi-linear MCSs in March through mid-April of 1998 is unique. However, Montroy (1997) has demonstrated that a statistically significant positive correlation exists between equatorial Pacific SSTs and precipitation in the south-central United States during the late stages of El Niño events. It is possible that in previous El Niño events large, quasi-linear MCS were connected to precipitation anomalies as in March through mid-April of 1998. We suggest as an area of future exploratory research an emphasis on heavy precipitation events during the warm seasons of El Niño, which might further connect the results of statistical studies to those of MCS summaries.

d. Episodic low-level wind features for March and April

A linkage between anomalies in equatorial Pacific SST and central U.S. precipitation in March through mid-April 1998 appears plausible, since El Niño influenced the extratropical jet stream, the jet stream affected the development of PECS, and the PECS distribution affected the precipitation anomalies. However, PECSs are dependent on transient weather conditions, so that analysis of the time-mean circulation provides only partial insight into how persistent features shaped the immediate environment of PECS. In order to build a meaningful measure of the transient flow we note that Anderson and Arritt (1998) found that PECS develop in regions of strong southerly flow, similar to MCCs for which low-level warm advection contributes mesoscale ascent and thermodynamic support (Cotton et al. 1989). In accordance with this finding, we have determined the frequency of northerly (NWE) and southerly wind events (SWE) from NPN observations and have created a time series of normalized coverage for both wind categories (see section 2c for definition of wind event). NWE (SWE) normalized coverage is defined as the percentage of reporting NPN stations that are categorized as NWE (SWE). We have smoothed the time series with a 5-h running average centered on the plotted hour. Half or more of the NPN sites must report in order for that hour to be included in the time series.

Time series of normalized coverage contain irregular oscillations between extensive SWE and NWE coverage through April of both years (Fig. 5). In 1997, these oscillations are more frequent in March to mid-April, when at least seven episodes of greater than 0.7 NWE coverage are observed, compared to about three in 1998. We have viewed 0000 and 1200 UTC 850-

hPa and surface maps and have found that periods of NWE coverage of 0.7 or greater are associated with southward moving cold fronts as a synoptic-scale low pressure system moves over the northeastern United States.

It is clear from Fig. 5 that PECS frequency is inversely related to NWE coverage. In particular, PECSs are infrequent when NWE coverage exceeds 0.7. Those that do occur when this threshold is exceeded are situated near the Gulf coast. As cold air spreads over the central United States during NWE outbreaks, the thermodynamic energy within the boundary layer becomes limited and vertical stratification becomes strongly stable. Favorable conditions return either by warming and moistening of boundary layer air from the surface or by replacement by advection. The latter scenario is more likely during spring months, since the solar zenith angle is relatively low, thereby limiting the amount of evapotranspiration that may occur. This inference has support in Fig. 5 as PECS development usually is delayed after NWE outbreaks until SWE coverage exceeds NWE coverage. Frequent peaks above the 0.7 NWE threshold in March 1997 indicate that the large-scale circulation guided synoptic-scale pressure systems across the United States in such a way as to cause bursts of cold air to move southward and suppress PECS development. In contrast, the active PECS period in March to early April of 1998 is characterized by persistent southerly low-level flow (Figs. 5c and 5d). As in March 1997, peaks of NWE coverage in 1998 are associated with the passage of synoptic-scale pressure systems through the central United States, but are less frequent even though the frequency of synoptic-scale systems is about the same or slightly greater than in 1997.

4. Conclusions

MCC and PECS were documented during the 1997–98 El Niño. Their time–latitude distributions followed climatological trends during the incipient stages of El Niño, while deviations from climatology were evident late in the El Niño event. PECSs were abnormally frequent in the Midwest in March and early April of 1998, when cold air outbreaks were infrequent despite the passage of several synoptic-scale pressure systems. MCCs during the summer of 1998 did not follow a typical northward migration but instead were clustered near 37°N, along the periphery of a tropospheric ridge that persisted from mid-May through the summer.

Positive precipitation anomalies and densely spaced MCS tracks were coincident over the central United States in every season, while negative precipitation anomalies occurred where MCS tracks were sparse. Of particular interest were the positive precipitation anomalies in summer 1997 and spring 1998, since these

anomalies are similar to statistically significant patterns associated with ENSO found in other studies. The additional documentation provided herein is offered as a possible starting point for more detailed study of dynamical linkages between ENSO, MCSs, and precipitation.

Acknowledgments. This research was sponsored by National Science Foundation Grants ATM-9616728 and ATM-9909650. This is Journal Paper Number J-19018 of the Iowa Agriculture and Home Economics Experiment Station, Project Number 3803, supported by Hatch Act and State of Iowa funds.

APPENDIX
Detailed Information on Mesoscale Convective Systems for 1997 and 1998

TABLE A1a. PECS events for 1997.

Initiation				Maximum					Termination			
Julian day	Time (UTC)	Lat (°)	Long (°)	Julian day	Time (UTC)	Lat (°)	Long (°)	Area (km ²)	Julian Day	Time (UTC)	Lat (°)	Long (°)
060	0100	36.93	-87.26	060	1300	37.80	-84.31	172600	060	1800	38.55	-85.09
060	1900	38.74	-84.34	061	0300	38.25	-85.83	206304	061	0700	36.61	-86.87
077	2000	29.13	-95.89	078	0200	32.96	-90.59	318767	078	1200	37.15	-82.90
084	0000	39.96	-93.09	084	0800	35.85	-95.31	202952	084	1300	39.08	-89.53
085	0700	29.75	-92.34	085	2000	27.18	-88.64	93903	085	2200	26.51	-89.73
094	0700	26.29	-98.16	094	1100	27.02	-96.33	83529	094	1300	33.53	-98.86
094	0700	30.16	-96.70	094	0900	31.69	-95.45	177101	094	1300	35.86	-92.71
094	2200	33.24	-93.69	095	1500	31.36	-90.58	259907	095	2000	33.08	-87.75
100	2300	34.87	-100.66	101	0700	36.77	-97.98	298259	101	1400	33.61	-96.14
111	0100	33.82	-96.43	111	0300	33.69	-95.60	210790	111	0700	31.47	-94.41
112	2200	32.08	-89.67	112	2300	32.33	-88.25	90564	113	0300	32.78	-84.57
113	0600	31.65	-84.84	113	1000	31.06	-82.19	109626	113	1800	28.17	-82.04
114	0900	35.69	-102.46	114	1300	35.60	-100.56	74037	114	1800	35.43	-96.59
115	0200	34.55	-100.45	116	0300	32.50	-91.48	433867	116	1300	31.74	-87.41
116	0100	30.05	-85.16	116	0800	28.27	-83.23	88783	116	1900	29.14	-80.85
116	1400	30.57	-88.61	116	1900	30.78	-87.78	370653	117	0200	29.92	-85.49
117	0600	31.81	-90.55	117	1600	31.58	-88.52	185139	118	0000	33.05	-83.52
118	0700	27.76	-84.52	118	1000	28.31	-82.97	137138	118	1800	26.59	-80.89
119	2300	40.25	-99.11	120	0000	40.61	-98.50	115010	120	0900	41.12	-94.79
122	0000	38.45	-98.69	122	0500	37.88	-96.28	206411	122	1000	36.78	-94.81
122	1500	32.69	-93.30	123	0300	34.53	-87.98	192028	123	0800	34.92	-85.64
123	0800	31.16	-90.26	123	1200	31.01	-88.02	148424	123	1800	32.08	-82.25
127	1000	39.55	-95.66	127	1200	41.03	-94.02	148424	127	1600	43.35	-92.98
127	2200	40.82	-94.38	128	0300	37.77	-94.82	453461	128	1200	41.10	-85.00
129	0000	34.51	-101.64	129	0500	34.23	-98.63	301210	129	1300	29.58	-100.19
129	1700	28.30	-98.23	129	2100	28.65	-96.55	119855	129	2300	29.10	-95.17
135	0600	32.13	-100.93	135	1000	31.91	-100.21	99698	135	1200	32.72	-97.96
136	0000	29.99	-98.52	136	0200	28.70	-97.61	186577	136	0900	28.55	-95.85
138	0100	38.39	-95.70	138	0400	38.09	-93.17	134732	138	0800	38.44	-89.38
139	0000	42.39	-88.63	139	0400	39.92	-91.93	445962	139	1700	34.09	-95.94
139	2200	31.74	-99.52	140	0200	31.49	-99.16	230563	140	1100	30.16	-96.76
140	2200	31.62	-93.34	141	0000	32.11	-92.33	80943	141	0300	32.46	-89.53
142	0400	27.80	-99.98	142	0700	28.43	-100.39	110400	142	1100	30.59	-101.03
142	2000	27.94	-96.18	142	2100	28.16	-96.02	116198	143	0200	29.62	-93.94
143	0400	28.09	-100.67	143	0900	28.00	-99.32	88462	143	1300	29.55	-98.95
143	1600	27.74	-96.88	143	1900	28.86	-95.66	60587	143	2300	31.70	-95.64
144	2100	31.00	-95.78	144	2300	31.03	-95.14	88724	145	0100	31.24	-93.09
144	2200	42.65	-104.31	145	0200	40.67	-102.52	304427	145	0900	42.97	-103.86
145	0900	36.60	-98.73	145	1000	36.52	-98.16	86615	145	1600	35.78	-94.57
145	0500	29.79	-90.23	145	0800	30.62	-88.73	110663	145	1400	30.20	-85.98
146	1200	37.22	-88.60	146	1400	36.83	-87.40	74534	146	1800	36.17	-85.32
146	2200	37.12	-88.74	147	0700	35.86	-91.03	484014	147	1600	35.36	-84.66
147	1800	32.44	-83.82	147	2100	31.35	-82.59	128346	148	0400	27.99	-80.62
147	2100	31.59	-96.66	148	0400	30.98	-96.43	532005	148	1200	31.46	-86.56
149	2200	37.35	-98.16	150	0600	34.40	-98.87	222762	150	1800	38.47	-90.36
150	2300	34.33	-94.21	151	0100	32.90	-94.87	135428	151	1000	28.88	-96.36
152	2200	42.70	-104.13	153	0500	42.29	-101.12	334193	153	1400	37.51	-98.35
154	0000	41.80	-102.64	154	0500	42.27	-100.63	127982	154	1000	42.43	-99.30
154	1100	38.64	-100.12	154	1300	37.90	-98.87	79213	154	1700	35.31	-97.96
157	0100	45.75	-109.20	157	0500	46.47	-108.55	94782	157	1100	48.00	-107.34
157	1000	33.17	-100.72	158	0100	29.47	-97.82	163285	158	0500	28.21	-99.00
157	2200	42.09	-106.48	158	0000	41.08	-105.64	142103	158	0400	44.73	-106.09
159	0900	35.28	-102.85	159	1500	33.84	-100.62	93862	159	1800	32.83	-99.43
159	2100	44.58	-107.51	160	0200	46.18	-107.29	116213	160	0500	48.21	-105.63
165	0100	33.53	-93.77	165	0300	33.09	-93.32	72448	165	0800	31.78	-93.98
165	2200	42.68	-105.77	166	0500	31.09	-98.18	290982	data unavailable			
167	1800	35.01	-89.29	167	2100	34.32	-86.80	76512	167	2300	33.80	-85.08
168	0100	34.96	-93.99	168	1100	34.71	-90.81	251478	168	1400	34.57	-89.26

TABLE 1a. (Continued)

Initiation				Maximum					Termination			
Julian day	Time (UTC)	Lat (°)	Long (°)	Julian day	Time (UTC)	Lat (°)	Long (°)	Area (km ²)	Julian Day	Time (UTC)	Lat (°)	Long (°)
168	1500	30.84	-90.06	168	1900	31.40	-88.19	237763	169	0100	31.89	-81.03
169	0000	27.66	-97.34	169	0100	27.69	-96.76	133330	169	1100	26.18	-97.34
169	0900	30.24	-89.95	169	1200	30.32	-89.45	118568	169	2000	28.21	-89.85
170	2300	41.84	-101.30	171	1200	43.79	-91.52	229532	171	1600	43.20	-90.01
171	2300	42.39	-101.86	172	0800	42.76	-92.51	593092	172	1700	44.24	-84.68
172	2300	40.96	-86.09	173	0300	39.17	-86.85	208559	173	1600	39.80	-91.66
174	0400	47.63	-102.86	174	0600	47.77	-99.85	111567	174	1000	47.47	-94.23
176	0100	38.43	-101.23	176	0500	40.11	-97.89	148961	176	0900	40.42	-93.72
179	0400	47.85	-93.83	179	0700	47.58	-93.79	78784	179	1100	47.36	-93.28
180	0000	45.17	-105.25	180	0300	46.59	-104.85	143345	180	0700	47.17	-101.96
180	0800	46.02	-93.56	180	1200	45.09	-95.14	130979	180	1800	43.41	-95.51
180	2300	47.06	-108.79	181	0200	47.51	-106.07	123107	181	1600	45.66	-97.79
181	0000	37.65	-96.76	181	0300	37.19	-95.53	141892	181	0600	36.57	-95.57
186	2200	38.72	-100.66	187	0100	36.97	-100.10	171431	187	0400	33.97	-101.21
188	0100	46.31	-106.44	188	0700	45.49	-101.54	105999	188	1500	46.00	-94.57
189	0000	42.60	-95.57	189	0300	42.00	-95.09	142475	189	1400	37.60	-94.01
190	0400	41.36	-101.86	190	0600	39.77	-101.14	87355	190	1100	41.43	-99.96
191	2100	35.21	-92.65	191	2300	35.10	-98.95	126371	192	0400	35.27	-97.06
193	0100	43.08	-100.57	193	0400	43.86	-99.67	141236	193	0900	43.80	-97.33
195	2100	40.62	-88.08	195	2300	39.68	-87.76	127598	196	0800	34.89	-90.31
198	0300	44.83	-98.64	198	0800	44.47	-93.50	168846	198	1400	43.45	-88.53
200	2100	41.10	-104.11	201	0100	40.96	-102.74	133092	201	1100	37.96	-97.78
200	2100	41.10	-104.11	201	0100	40.96	-102.74	133092	201	0800	44.78	-98.75
202	0200	37.22	-102.15	202	0600	36.58	-100.49	78628	202	0800	36.88	-99.20
204	2000	31.46	-90.97	205	0000	31.81	-91.62	171278	205	0300	31.65	-94.16
208	0300	40.62	-83.19	208	0400	40.13	-83.01	90605	208	1000	36.73	-81.93
208	1600	43.62	-96.12	209	0200	40.33	-95.47	272716	209	1100	38.91	-96.68
209	2100	36.83	-85.04	209	2300	36.57	-87.19	204579	210	0300	35.79	-88.52
209	2300	36.76	-103.14	210	0300	37.72	-102.76	112384	210	0800	38.66	-102.43
210	2000	34.34	-94.55	211	0100	32.33	-91.74	91778	211	0400	31.43	-93.08
220	0000	47.69	-110.94	220	0400	47.05	-109.44	71450	220	0600	46.29	-108.82
222	2200	35.61	-101.57	223	0300	34.63	-99.55	160231	223	0900	36.21	-96.74
228	2200	42.15	-83.18	229	0600	41.46	-91.54	355972	229	1600	35.26	-95.50
230	0100	34.36	-97.87	230	0300	34.19	-98.39	60650	230	0700	33.46	-99.51
231	0000	33.44	-101.36	231	0300	34.55	-99.93	171186	231	0900	35.20	-96.61
231	2200	36.70	-88.32	232	0000	36.43	-87.99	92462	232	0600	35.95	-86.53
244	0000	46.90	-97.14	244	0300	46.69	-96.89	109509	244	1000	46.95	-94.18
250	0000	44.36	-98.96	250	0200	42.92	-98.74	145140	250	0800	43.07	-94.31
251	2100	43.27	-96.24	252	0000	41.99	-97.39	82438	252	0300	40.51	-96.98
252	2200	30.52	-93.78	253	0000	29.79	-93.61	102459	253	0300	28.33	-94.38
259	0100	47.76	-103.88	259	0300	48.02	-101.82	65022	259	0900	47.82	-95.84
259	1200	45.83	-94.98	260	0200	42.73	-88.16	232697	260	0900	38.67	-89.92
266	2200	27.89	-97.34	267	0700	26.32	-96.22	146093	267	0800	26.23	-96.02

TABLE A1b. PECS events for 1998.

Initiation				Maximum					Termination			
Julian day	Time (UTC)	Lat (°)	Long (°)	Julian day	Time (UTC)	Lat (°)	Long (°)	Area (km ²)	Julian Day	Time (UTC)	Lat (°)	Long (°)
065	2200	29.44	-88.62	066	0300	30.53	-86.45	173568	066	1000	33.16	-84.50
066	1000	30.53	-88.74	066	1700	31.77	-88.28	208334	066	2100	31.30	-91.80
066	1000	34.15	-98.70	066	2200	34.57	-90.97	322408	067	1200	32.59	-84.23
067	0300	40.58	-93.44	067	0700	40.65	-90.79	119585	067	1100	42.74	-90.47
067	2100	32.95	-83.09	068	0000	33.47	-83.04	206178	068	0700	26.77	-81.23
068	0700	40.56	-82.58	068	0700	40.56	-82.58	89602	068	1200	43.83	-82.13
074	1900	34.96	-101.51	075	1700	33.49	-93.90	440429	077	0700	26.87	-82.96
076	0000	39.89	-99.16	076	0300	40.48	-97.57	133923	076	1300	42.95	-92.92
076	0300	35.16	-87.02	076	0700	36.00	-84.19	84901	076	0900	35.58	-83.12
077	1200	28.68	-88.60	077	2000	33.11	-84.24	337289	078	0700	34.61	-80.81
078	0700	36.88	-95.52	078	1000	37.54	-94.03	116708	078	1400	37.65	-90.87
078	1700	37.80	-93.81	078	2000	38.00	-92.18	143186	079	0900	40.46	-83.31
086	0300	41.52	-100.50	086	1200	46.18	-92.71	80381	086	1500	47.23	-88.10
088	0200	42.67	-101.63	088	0300	43.09	-102.83	98353	088	1200	45.51	-98.52
088	2200	44.99	-91.30	089	0100	46.12	-87.54	185057	089	0300	46.27	-86.34
089	0700	40.17	-95.69	089	0900	41.49	-93.80	118430	089	1300	44.22	91.95
089	2100	41.96	-92.72	090	0300	42.17	-90.49	275037	090	1500	46.56	-84.85
097	0000	42.16	-94.86	097	0200	41.24	-94.72	143158	097	0700	41.17	-96.96
099	0100	34.13	-84.63	099	0300	34.93	-82.99	161881	099	0800	34.67	-81.55
102	0700	45.58	-104.96	102	1100	46.90	-99.54	153660	102	1700	47.04	-101.92
105	0000	41.40	-95.65	105	0200	41.85	-92.87	103264	105	0600	43.56	-90.21
106	0200	38.64	-87.00	106	0800	38.65	-85.02	124856	106	1300	37.22	-83.87
107	0100	35.07	-85.13	107	0300	35.63	-82.97	141063	107	0700	34.82	-81.56
109	1000	29.99	-86.58	109	1500	30.18	-84.55	191650	109	2000	29.04	-84.03
118	0000	33.61	-91.41	118	0600	33.51	-89.61	184177	118	1800	36.38	-85.54
118	1800	29.22	-89.04	119	1400	29.03	-88.55	197063	119	2300	27.51	-87.88
127	0400	36.57	-89.43	127	1000	36.47	-85.23	145242	127	1400	35.67	-82.38
132	0100	41.09	-97.56	132	0400	41.41	-96.04	136343	132	0900	40.43	-92.35
135	2200	45.96	-93.71	136	0200	45.45	-90.28	101647	136	0500	44.32	-87.78
141	0800	39.22	-104.88	141	1000	36.67	-102.44	105918	141	1500	34.95	-98.98
141	1300	42.00	-100.94	141	1500	42.47	-100.03	122441	141	2100	42.24	-95.27
141	1800	39.16	-90.22	142	0100	37.00	-88.02	162885	142	0700	36.15	-86.49
142	0100	41.21	-100.09	142	0700	41.93	-96.24	143287	142	2000	38.60	-85.01
142	0700	40.26	-90.57	142	0800	41.11	-92.75	219423	142	1600	37.49	-84.56
143	0400	39.39	-86.97	143	0600	39.34	-84.85	98717	143	1200	37.96	-81.55
143	2200	38.52	-90.17	144	0000	39.62	-89.52	98743	144	0900	37.91	-81.76
146	0300	33.44	-99.15	146	1000	35.56	-95.45	228555	146	1600	35.56	-89.27
147	0000	44.45	-105.56	147	0200	43.58	-104.04	130891	147	0600	44.54	-102.18
148	2300	43.04	-92.26	149	0700	42.09	-93.20	222306	149	1500	38.12	-92.68
149	2200	43.30	-104.46	150	0400	43.36	-100.41	112947	150	2200	40.93	-89.07
150	0500	47.48	-105.52	150	1200	46.94	-94.04	119486	150	1700	46.76	-89.70
150	1200	40.13	-101.61	150	1300	40.51	-101.60	78540	150	1900	41.26	-99.85
156	0000	33.22	-97.29	156	0500	34.44	-93.26	203354	156	1200	34.72	-84.71
156	2300	30.94	-95.25	157	0200	31.45	-92.21	188062	157	0800	31.85	-85.26
158	2300	40.86	-101.91	159	0300	42.04	-98.43	134320	159	0700	42.70	-95.19
158	2300	33.33	-97.61	159	0500	36.07	-94.39	155425	159	0800	34.07	-92.45
159	0700	39.30	-100.38	159	1500	38.07	-92.66	220651	160	0400	36.51	-86.71
162	0400	31.39	-100.12	162	0700	33.23	-97.52	219595	162	1400	39.39	-89.00
163	2200	41.31	-84.14	164	0100	39.29	-84.73	115161	164	0500	37.54	-84.46
164	2300	42.93	-101.15	165	0000	43.34	-101.02	105889	165	0600	40.55	-92.70
168	0100	42.49	-104.54	168	0800	43.82	-98.86	257181	168	2100	41.80	-89.84
169	0200	42.68	-98.52	169	0600	45.07	-98.44	223150	169	1500	46.25	-91.47
169	1500	40.63	-91.75	169	1800	42.76	-90.85	107870	169	2100	43.46	-88.87
169	2000	41.31	-93.56	170	0500	37.29	-91.01	324366	170	1000	36.69	-87.85
170	1600	34.67	-85.02	170	2000	33.38	-83.13	163099	171	0100	30.64	-81.56
172	0000	40.89	-94.34	172	0200	40.80	-93.32	98465	172	0800	38.74	-88.79
176	0500	44.94	-95.92	176	0900	45.64	-90.20	83378	176	1200	45.09	-86.77
177	1900	47.18	-99.85	178	0500	45.35	-92.47	190427	178	1200	43.37	-85.70
178	2300	44.40	-93.38	179	0500	42.87	-90.82	366841	179	1100	41.31	-86.49
180	0200	38.93	-94.53	180	0600	39.18	-92.58	262271	180	1300	38.50	-91.33
180	1900	42.02	-92.93	181	0400	38.40	-89.74	314862	181	1300	37.07	-93.94
184	0700	43.23	-101.24	184	1200	42.43	-95.87	70380	184	1500	41.72	-93.88
187	2100	43.17	-97.75	188	0300	40.52	-96.07	215330	188	1300	38.48	-86.74
190	0400	37.04	-102.67	190	0600	38.49	-101.36	72378	190	1200	38.26	-97.44
190	1900	30.09	-84.84	191	0100	31.40	-86.12	248785	191	0400	29.96	-87.33

TABLE A1b. (Continued)

Initiation				Maximum					Termination			
Julian day	Time (UTC)	Lat (°)	Long (°)	Julian day	Time (UTC)	Lat (°)	Long (°)	Area (km ²)	Julian Day	Time (UTC)	Lat (°)	Long (°)
191	0400	39.90	-101.57	191	0800	39.78	-99.18	72170	191	1000	40.01	-96.94
191	2100	34.33	-89.29	191	0000	32.01	-88.59	248785	192	0400	31.80	-89.75
193	1600	26.59	-84.37	192	2200	27.95	-81.79	72170	194	0100	26.72	-80.52
201	0000	41.03	-83.97	193	0700	39.47	-83.12	87556	201	1200	38.70	-84.86
203	0100	42.24	-84.82	203	0800	41.44	-87.23	135660	203	1200	41.11	-85.15
203	0100	40.94	-102.35	203	0600	41.68	-95.70	250132	203	1000	41.01	-95.76
203	2200	40.04	-86.99	204	0100	39.56	-87.24	127420	204	0400	38.46	-88.04
205	2000	34.64	-88.27	205	2300	32.82	-86.64	182788	206	0400	32.92	-90.71
206	2300	41.16	-103.29	207	1100	39.02	-94.02	168396	207	1500	37.76	-91.13
208	0900	36.84	-89.89	208	1200	36.40	-88.73	134423	208	1500	34.93	-87.84
211	0000	40.17	-101.37	211	0800	39.02	-99.05	160235	211	1000	39.20	-98.24
211	0700	36.38	-89.72	211	1100	37.29	-89.26	122112	211	1500	38.69	-88.89
224	2000	32.29	-88.27	224	2200	32.13	-87.72	134774	225	0200	31.34	-85.35
226	1900	29.67	-99.57	227	0000	27.70	-98.28	119861	227	0500	25.88	-98.83
229	0300	47.37	-91.94	229	0600	47.23	-89.85	65849	229	1300	42.64	-90.75
234	0100	28.04	-95.29	234	1000	28.74	-96.30	120140	234	1800	28.56	-94.62
240	0000	38.46	-98.44	240	0300	38.95	-97.46	127920	240	0900	34.75	-101.25

TABLE A2a. MCC events for 1997.

Initiation				Maximum					Termination			
Julian day	Time (UTC)	Lat (°)	Long (°)	Julian day	Time (UTC)	Lat (°)	Long (°)	Area (km ²)	Julian Day	Time (UTC)	Lat (°)	Long (°)
083	1000	41.24	-97.28	083	1600	41.84	-92.46	104342	083	2000	42.94	-90.94
083	2000	40.26	-89.00	083	2200	41.45	-87.50	97520	084	0300	42.59	-82.23
101	0800	30.39	-95.43	101	1500	30.27	-91.30	182662	102	0200	29.35	-86.57
102	1000	30.88	-90.04	102	1500	29.45	-86.98	145606	102	2200	26.96	-85.88
112	0700	34.70	-99.01	112	1500	33.57	-91.70	164448	113	0100	33.98	-81.50
116	0600	29.23	-99.25	116	0900	30.52	-98.39	138815	116	1700	34.81	-95.93
127	0100	36.36	-101.60	127	0500	36.13	-98.77	194151	127	0900	36.95	-96.56
146	0000	34.64	-96.23	146	0300	33.87	-95.14	78401	146	0600	33.74	-94.04
146	0100	38.72	-97.03	146	0400	38.20	-94.80	89288	146	0800	38.57	-91.84
163	2300	38.09	-101.65	164	0800	37.42	-96.26	172407	164	1700	38.53	-88.65
171	2100	31.27	-86.58	172	0000	31.79	-87.18	90159	172	0700	33.25	-88.73
172	2100	29.69	-96.36	173	0000	29.61	-96.55	100689	173	0400	30.67	-94.19
174	0000	44.79	-95.35	174	0300	44.08	-93.03	106717	174	0600	43.11	-90.80
179	1500	46.69	-98.10	179	2300	46.05	-92.70	159021	180	0700	45.95	-93.33
190	0100	38.04	-98.43	190	0800	37.74	-93.65	155999	190	0900	37.59	-93.90
192	0100	47.42	-102.80	192	0400	47.66	-101.28	79579	192	0700	47.34	-98.15
198	0000	44.18	-87.15	198	0100	44.12	-86.95	134075	198	0600	43.51	-86.44
199	0100	47.97	-106.90	199	1400	45.85	-96.56	150188	199	2300	40.59	-86.61
199	0400	36.45	-96.41	199	0800	36.27	-96.93	56167	199	1000	35.95	-96.53
200	0000	44.20	-104.47	200	0600	45.02	-103.00	168084	200	0900	44.64	-99.65
200	1300	45.24	-94.40	200	1600	44.92	-92.68	90306	200	2100	42.21	-90.11
203	0200	26.96	-99.96	203	0500	28.20	-100.04	83982	203	0700	28.87	-100.08
205	0200	43.70	-102.23	205	0600	44.30	-100.10	154166	205	1300	44.57	-94.39
206	0500	44.66	-96.37	206	1000	45.29	-92.55	165831	206	1700	43.04	-88.67
208	2100	41.10	-84.83	209	0000	39.80	-83.36	77016	209	0300	38.97	-81.74
218	1300	37.96	-99.14	218	1500	37.56	-98.24	68997	218	1900	37.07	-96.44
221	0400	46.11	-102.34	221	0700	46.53	-99.89	83958	221	1300	45.94	-97.09
222	0600	37.52	-101.77	222	1000	38.39	-99.25	88990	222	1300	39.55	-98.73
224	0500	37.94	-101.84	224	1100	37.11	-98.74	100243	224	1400	37.38	-96.43
234	0300	39.62	-99.14	234	0700	38.09	-97.13	148014	234	1300	34.34	-96.02
240	0300	48.23	-103.89	240	0900	47.64	-103.06	66139	240	1100	47.03	-101.76
242	0000	44.19	-96.77	242	0900	44.57	-91.49	82717	242	1100	43.05	-90.81

TABLE A2b. MCC event for 1998.

Initiation				Maximum					Termination			
Julian day	Time (UTC)	Lat (°)	Long (°)	Julian day	Time (UTC)	Lat (°)	Long (°)	Area (km ²)	Julian Day	Time (UTC)	Lat (°)	Long (°)
135	0700	35.42	-100.60	135	1300	39.85	-95.89	138610	135	1700	44.47	-93.53
137	0200	30.09	-101.00	137	0600	30.40	-100.71	91564	137	1200	31.91	-100.19
139	0200	38.61	-99.31	139	0600	39.18	-97.73	107837	139	0900	38.80	-96.42
139	2300	40.55	-87.39	140	0300	39.52	-85.40	209970	140	0800	37.50	-81.93
140	0000	42.66	-102.45	140	0400	42.67	-99.45	184739	140	1700	41.63	-91.38
144	0100	40.60	-92.41	144	0400	41.97	-91.54	155334	144	0700	42.78	-88.02
145	0000	38.37	-97.73	145	0600	37.83	-94.71	260519	145	1000	36.73	-92.75
147	0000	32.98	-101.81	147	0800	32.67	-99.06	239048	147	1200	34.01	-95.10
148	0800	45.73	-91.02	148	1200	44.61	-87.09	103257	148	1400	43.10	-86.75
151	0100	45.24	-95.64	151	0800	44.84	-86.52	202421	151	1300	42.88	-82.00
151	2200	37.85	-84.62	152	0600	34.98	-82.94	145918	152	1100	33.48	-83.51
160	0300	35.75	-93.96	160	0900	37.11	-88.32	251043	160	1800	36.27	-81.86
160	2300	34.54	-97.32	161	0200	34.93	-94.75	140803	161	0800	35.28	-93.37
164	2300	37.20	-95.86	165	0200	36.58	-93.05	163035	165	0600	36.76	-88.92
171	0300	37.82	-92.94	171	1100	38.15	-90.25	205961	171	1600	37.26	-90.10
188	2100	38.98	-87.58	189	0000	38.19	-85.68	104270	189	0300	37.68	-83.44
188	2300	36.13	-102.89	189	0400	37.34	-101.41	178826	189	1200	37.44	-95.35
200	0100	44.65	-97.42	200	0500	43.97	-93.29	154204	200	1200	42.18	-87.21
205	0400	38.30	-102.75	205	0600	38.75	-101.15	75981	205	1100	38.55	-98.11
206	0100	38.80	-103.13	206	0300	38.88	-102.71	101554	206	1100	38.64	-97.65
212	0100	36.82	-89.10	212	0400	36.58	-87.66	106217	212	0700	36.22	-87.59
212	0200	35.39	-103.12	212	0600	36.56	-102.26	106411	212	0900	36.86	-101.14
214	0300	39.18	-101.22	214	0500	39.49	-99.75	82153	214	1200	39.56	-95.47
222	2200	35.01	-99.24	223	0300	35.85	-101.33	116816	223	0700	37.04	-100.46
223	0000	36.93	-91.03	223	0300	36.64	-89.84	75561	223	0600	35.51	-89.09
228	2100	29.25	-99.44	229	0400	27.75	-98.73	107366	229	0900	26.85	-99.30
234	0300	47.35	-100.54	234	1000	46.81	-95.44	105383	234	1400	45.87	-91.53
236	0600	29.89	-100.54	236	0900	29.70	-100.42	82502	236	1300	29.89	-100.54
250	0700	41.70	-86.09	250	1000	41.31	-84.14	130714	250	1200	39.83	-81.46

REFERENCES

- Anderson, C. J., and R. W. Arritt, 1998: Mesoscale convective complexes and persistent elongated convective systems over the United States during 1992 and 1993. *Mon. Wea. Rev.*, **126**, 578–599.
- Arritt, R. W., T. D. Rink, M. Segal, D. P. Todey, C. A. Clark, M. J. Mitchell, and K. M. Labas, 1997: The Great Plains low-level jet during the warm season of 1993. *Mon. Wea. Rev.*, **125**, 2176–2192.
- Augustine, J. A., 1985: An automated method for the documentation of cloud-top characteristics of mesoscale convective systems. NOAA Tech. Memo. ERL ESG-10, NOAA/FSL, Boulder, CO, 121 pp. [Available from NOAA/FSL, 325 Broadway, Boulder, CO 80303.]
- , and K. W. Howard, 1988: Mesoscale convective complexes over the United States during 1985. *Mon. Wea. Rev.*, **116**, 685–701.
- , and —, 1991: Mesoscale convective complexes over the United States during 1986 and 1987. *Mon. Wea. Rev.*, **119**, 1575–1589.
- Barnes, S. L., 1964: A technique for maximizing details in numerical weather maps. *J. Appl. Meteor.*, **3**, 396–409.
- Barnston, A. G., A. Leetmaa, V. E. Kousky, R. E. Livezey, E. A. O'Lenic, H. Van den Dool, A. J. Wagner, and D. A. Unger, 1999: NCEP forecasts of the El Niño of 1997–98 and its U.S. impacts. *Bull. Amer. Meteor. Soc.*, **80**, 1829–1852.
- Bartels, D. L., J. M. Skradski, and R. D. Menard, 1984: Mesoscale convective systems: A satellite data-based climatology. NOAA Tech. Memo. ERL ESG 8, 63 pp. [NTIS PB-85-187904.]
- Bell, G. D., and M. S. Halpert, 1998: Climate assessment for 1997. *Bull. Amer. Meteor. Soc.*, **79** (May), S1–S50.
- , —, C. F. Ropelewski, V. E. Kousky, A. V. Douglas, R. C. Schnell, and M. E. Gelman, 1999: Climate assessment for 1998. *Bull. Amer. Meteor. Soc.*, **80** (May), S1–S48.
- Bunkers, M. J., J. R. Miller Jr., and A. T. DeGaetano, 1996: An examination of El Niño–La Niña-related precipitation and temperature anomalies across the northern plains. *J. Climate*, **9**, 147–160.
- Cotton, W. R., M.-S. Lin, R. L. McAnnelly, and C. J. Treback, 1989: A composite model of mesoscale convective complexes. *Mon. Wea. Rev.*, **117**, 765–783.
- Daniel, C. J., R. W. Arritt, and C. J. Anderson, 1999: Accuracy of 404-MHz radar profilers for detection of low-level jets over the central United States. *J. Appl. Meteor.*, **38**, 1391–1399.
- Fritsch, J. M., R. J. Kane, and C. R. Chelius, 1986: The contribution of mesoscale convective weather systems to the warm-season precipitation in the United States. *J. Climate Appl. Meteor.*, **25**, 1333–1345.
- Horel, J. D., and J. M. Wallace, 1981: Planetary-scale atmospheric phenomena associated with the Southern Oscillation. *Mon. Wea. Rev.*, **109**, 813–829.
- Kalnay, E., and Coauthors, 1996: The NCEP/NCAR 40-Year Reanalysis Project. *Bull. Amer. Meteor. Soc.*, **77**, 437–471.
- Kunkel, K. E., S. A. Chagnon, and J. R. Angel, 1994: Climatic aspects of the 1993 upper Mississippi River basin flood. *Bull. Amer. Meteor. Soc.*, **75**, 811–822.
- Laing, A. G., and J. M. Fritsch, 1997: The global population of mesoscale convective complexes. *Quart. J. Roy. Meteor. Soc.*, **123**, 389–405.
- Maddox, R. A., 1980: Mesoscale convective complexes. *Bull. Amer. Meteor. Soc.*, **61**, 1374–1387.
- , 1983: Large-scale meteorological conditions associated with midlatitude, mesoscale convective complexes. *Mon. Wea. Rev.*, **111**, 1475–1493.

- McPhadden, M. J., and X. Yu, 1999: Genesis and evolution of the 1997–98 El Niño. *Science*, **283**, 950–954.
- Mitchell, M. J., R. W. Arritt, and K. Labas, 1995: A climatology of the warm season Great Plains low-level jet using wind profiler observations. *Wea. Forecasting*, **10**, 576–591.
- Mo, K. C., J. N. Paegle, and R. W. Higgins, 1997: Atmospheric processes associated with summer floods and droughts in the central United States. *J. Climate*, **10**, 3028–3046.
- Montroy, D. L., 1997: Linear relation of central and eastern North American precipitation to tropical Pacific sea surface temperature anomalies. *J. Climate*, **10**, 541–558.
- Rasmussen, E. M., and K. Mo, 1993: Linkages between 200-mb tropical and extratropical circulation anomalies during the 1986–1989 ENSO cycle. *J. Climate*, **6**, 595–616.
- Rodgers, D. M., K. W. Howard, and E. C. Johnston, 1983: Mesoscale convective complexes over the United States during 1982. *Mon. Wea. Rev.*, **111**, 2363–2369.
- , M. J. Magnano, and J. H. Arns, 1985: Mesoscale convective complexes over the United States during 1983. *Mon. Wea. Rev.*, **113**, 888–901.
- Ropelewski, C. F., and M. S. Halpert, 1986: North American precipitation and temperature patterns associated with the El Niño/Southern Oscillation (ENSO). *Mon. Wea. Rev.*, **114**, 2352–2362.
- , and —, 1987: Global and regional scale precipitation patterns associated with the El Niño/Southern Oscillation. *Mon. Wea. Rev.*, **115**, 1606–1626.
- , and —, 1989: Precipitation patterns associated with the high index phase of the Southern Oscillation. *J. Climate*, **2**, 268–284.
- , and —, 1996: Quantifying Southern Oscillation–precipitation relationships. *J. Climate*, **9**, 1043–1059.
- Sardeshmukh, P. D., and B. J. Hoskins, 1988: The generation of global rotational flow by steady idealized tropical divergence. *J. Atmos. Sci.*, **45**, 1228–1251.
- Stensrud, D. J., 1996: Importance of low-level jets to climate: A review. *J. Climate*, **9**, 1698–1711.
- Ting, M., and H. Wang, 1997: Summertime U.S. precipitation variability and its relation to Pacific sea surface temperature. *J. Climate*, **10**, 1853–1873.
- Trenberth, K. E., 1997: Short-term climate variations: Recent accomplishments and issues for future progress. *Bull. Amer. Meteor. Soc.*, **78**, 1081–1096.
- Velasco, I., and J. M. Fritsch, 1987: Mesoscale convective complexes in the Americas. *J. Geophys. Res.*, **92**, 9591–9613.
- Wolter, K., and M. S. Timlin, 1998: Measuring the strength of ENSO—How does 1997/98 rank? *Weather*, **53**, 315–324.